

Article

Determination of Critical Damage Size of Inclined Waterproof Coal Pillar under Asymmetric Load

Xingping Lai ^{1,2}, Xiaoqian Yuchi ^{1,2,*} , Helong Gu ^{1,2}, Pengfei Shan ^{1,2}  and Wenhua Yang ^{1,2}

¹ College of Energy Science and Engineering, Xi'an University of Science and Technology, Xi'an 710054, China; laixp@xust.edu.cn (X.L.); helonggu@xust.edu.cn (H.G.); shanpengfei@xust.edu.cn (P.S.); b201512035@stu.xust.edu.cn (W.Y.)

² Key Laboratory of Western Mines and Hazard Prevention of China Ministry of Education, Xi'an University of Science and Technology, Xi'an 710054, China

* Correspondence: 13484519960@163.com

Abstract: Quantitative determination of the critical size of an inclined coal pillar in an old goaf water-affected area is of great significance for water damage prevention and safe mining. The critical size of the inclined waterproof coal pillar is derived by using mechanical analyses, numerical calculations, and field engineering practices to determine the stability of the waterproof coal pillar in the old goaf water-affected area of the 1303 working face of Dananhu No. 1 Mine in the Xinjiang region. Firstly, a force model of the inclined waterproof coal pillar was established to reveal the law that the critical size of the coal pillar increases with the increase in coal seam inclination under the action of asymmetric load. Then, numerical simulation was applied to reveal the dynamic evolution processes of plastic deformation–destabilization of the coal pillar under the influence of mining and single-side water pressure, and the critical size of the coal pillar in the study area was determined to be 19.09 m. Finally, measures such as pumping pressure relief and slurry reinforcement were adopted to reduce the deformation rate of the roadway on the side of the coal pillar, which ensured the stability of the waterproof coal pillar and the safe mining of the working face.

Keywords: inclined coal seam; asymmetric loading; waterproof coal pillar; critical size



Citation: Lai, X.; Yuchi, X.; Gu, H.; Shan, P.; Yang, W. Determination of Critical Damage Size of Inclined Waterproof Coal Pillar under Asymmetric Load. *Water* **2024**, *16*, 1233. <https://doi.org/10.3390/w16091233>

Academic Editor: Chin H. Wu

Received: 29 March 2024

Revised: 15 April 2024

Accepted: 22 April 2024

Published: 25 April 2024



Copyright: © 2024 by the authors. Licensee MDPI, Basel, Switzerland. This article is an open access article distributed under the terms and conditions of the Creative Commons Attribution (CC BY) license (<https://creativecommons.org/licenses/by/4.0/>).

1. Introduction

Over 60% of China's electricity is generated through coal combustion, making the secure and efficient extraction of coal resources vital to the nation's economic development. One key aspect of ensuring the safety of coal mining operations is the rational design and stability control of coal pillars [1–4]. Additionally, given China's complex underground hydrological conditions, with up to 25 billion tons of coal reserves affected by water, the design of many coal pillars must consider not only the safe bearing of overlying strata loads and the stability of surrounding roadways but also the prevention of water-related hazards in voids left by coal extraction [5,6]. However, coal pillars, as underground support structures, are inherently fraught with complexities due to their geological formation and the presence of numerous fractures [7–9]. Human-induced disturbances, such as mining activities, can easily weaken these structures internally [10,11]. When the load-bearing capacity of a coal pillar reaches its yield limit, catastrophic events like structural collapse are highly likely, resulting in significant economic losses and potentially even loss of life [12–14].

To address these issues, numerous scholars have conducted extensive research on waterproof coal pillars, yielding significant findings. For example, theories like load estimation methods have been used to analyze the characteristics of overlying strata loads on coal pillars, focusing on these loads as the primary source of instability and elucidating the mechanisms behind pillar failure [15,16]. For example, by drawing on the two-zone constraint theory, the waterproof coal pillar is divided into three parts, the central elastic

zone and the plastic zone on both sides, and using the relevant theory of elastic mechanics, the critical size formula of the elastic zone of the coal pillar in the near-horizontal coal seam under the combined effect of uniform load and water pressure is derived [17–20]. For example, using the theory of hydrodynamics and multiple regression [21–23], we analyze the reasonable width of the waterproof coal pillar under the influence of different types of faults and derive the formula for calculating the size of the waterproof coal pillar when the fault dip angle is large and small [24–27]. For example, neural networks and improved numerical calculation algorithms have been employed for reasonable analysis and prediction of coal pillar dimensions [28,29]. The analysis of the influence of the overburden collapse process and the development characteristics of the water-conducting fracture zone on the stability of the waterproof pillar is given using a physically similar simulation [30–35]. In recent years, with the widespread development of computers, numerical simulation has gradually become a new means to study the size of waterproof coal pillars [36–40]. Many scholars mostly use the seepage and deformation theory to establish the numerical model of solid-flow coupling in the coal seam mining process to reveal the stress evolution law of coal pillars of different widths under the influence of water and mining, which is used as the basis for the size of waterproof pillars [41–43].

On this basis, there is much research on the problem of coal pillar strength decline caused by inclination angle, and fruitful results have been achieved [44]. For example, starting with the shear action on one side of the coal pillar caused by the inclined coal seam, generalized Mohr circle research, applicable to inclined coal pillars, was carried out [45,46], and the energy dissipation characteristics of coal rock mass in sharply inclined mining were identified so as to analyze the influence of the coal seam inclination angle, lateral pressure coefficient, and the ratio of width and height on the ultimate strength of inclined section coal pillars. The disaster mechanism of inclined coal pillars was also obtained by combining the numerical simulation [47,48]. Although these results do not consider the role of coal pillars on the blocking water capacity, they deeply analyze the change in the overburden load of coal pillars caused by the coal seam inclination angle. They also consider the coupling relationship between coal seam characteristics and coal pillar structure. Therefore, these results have a good reference significance for determining the ultimate strength of inclined waterproof coal pillars.

Therefore, this paper focuses on the asymmetrical loading on inclined waterproof coal pillars caused by their angle of inclination. It examines the stress patterns and critical instability characteristics of the elastic barrier zone in inclined pillars, studies the dynamic evolution of plastic deformation–instability–failure of the inclined waterproof coal pillar under the influence of mining activities and unilateral water pressure, and establishes expressions for the critical failure dimensions of the inclined coal pillar under unilateral hydrostatic pressure. This provides a reference for the stability research of inclined coal pillars in similar geological conditions and offers scientific theoretical support for preventing disasters caused by underground space instability.

2. Mechanics Modeling

2.1. Force Analysis of Inclined Waterproof Coal Pillar

Artificial mining disturbance is the critical factor in breaking the balance of stress between the coal pillar and its surrounding rock and leading to the formation of old goaf water. In the actual production process, with the back mining of two working faces and the gradual generation of old goaf water in the mining area, both ends of the waterproof coal pillar are affected by the support pressure, and one side is also affected by old goaf water, which produces stress concentration in both sides of the coal pillar. When the degree of stress concentration exceeds the bearing capacity of the coal pillar body, the internal joint fracture of the coal pillar will gradually expand, resulting in the transformation of the structure of both sides of the coal pillar from the elastomeric to the plastic body. When the plastic zone on both sides expands to penetration, the coal pillar will lose its load-bearing and water-insulation capacity.

In this process, as the force characteristics along the direction of roadway advancement in the coal pillar change minimally, the cross-section of the coal pillar is typically the focus of study. This reveals that the ends of the coal pillar bear more load, leading to more fracture development and a transition from an elastic to a plastic state. Closer to the middle of the pillar, the overlying strata load approaches the original rock stress, resulting in less transformation between elastic and plastic states in the coal pillar.

Therefore, in this paper, the coal pillar under the influence of water addition in the mining area is divided into the mining disturbance zone (MDZ), the elastic barrier zone (EBZ), and the water pressure-affected zone (WAZ), as Figure 1 shows. In this figure, G is the overburden load (vertical direction) under mining disturbance; q is the hydrostatic pressure value on one side of the coal pillar; α is the inclination angle of the coal seam; and H is the height from the middle of the elastic zone of the coal pillar to the ground surface.

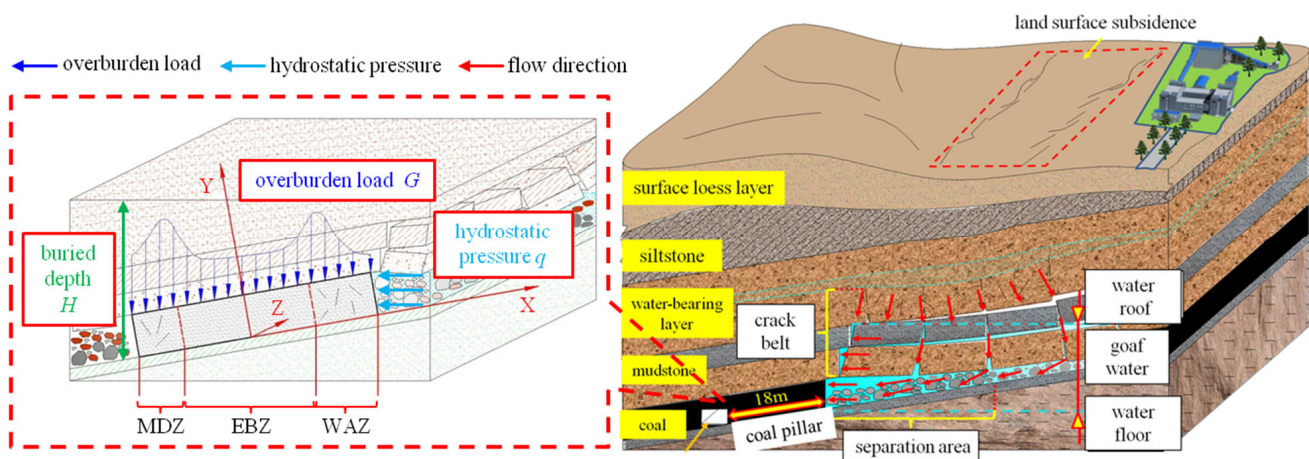


Figure 1. Overburden load of inclined waterproof coal pillar.

2.2. Determination of the Critical Length of the Elastic Barrier Zone

From the instability process of the overburden load on inclined pillars, it is inferred that the cross-sectional structure of an inclined pillar can be simplified into shorter mining-disturbed zones at both ends and a longer central elastic zone (EBZ). Since the bearing capacity of the plastic zones on both sides is compromised, the central elastic body should be the main focus of the study. Since the force direction in the elastic barrier area of the waterproof pillar is mainly concentrated in the XOY plane (Figure 1), and the force characteristics of the tangent plane perpendicular to the Z axis (parallel to the XOY plane) are similar, the force state of the coal pillar can be simplified to a plane problem for solution [49].

Assuming that the length of the elastic barrier zone (EBZ) is l , the overburden load of the coal pillar is G_0 , and the hydrostatic pressure q is constant after crossing the water pressure influence zone, a simplified model of the elastic barrier zone mechanics can be obtained, as shown in Figure 2a.

When the X-axis is in the horizontal direction and the Y-axis is in the vertical direction, σ_0 is the horizontal constraint between the coal body in the elastic zone and the water pressure influence zone; σ_3 is the horizontal constraint between the coal body in the elastic zone and the recovery disturbance zone; q is the hydrostatic pressure value after crossing the plastic zone of the coal pillar; and α is the dip angle of the coal seam. It is known from the literature [50,51] that the load on the elastic zone of the coal pillar will gradually increase with the mining of the working face. If the average volume force γ of the overburden on the coal pillar is defined and the vertical height from the middle of the coal pillar to the surface is H , the bearing pressure in the elastic zone of the coal pillar is approximately the constant $K_1 \gamma H$, where K_1 is the stress concentration factor of the elastic zone (generally half of the maximum stress concentration factor).

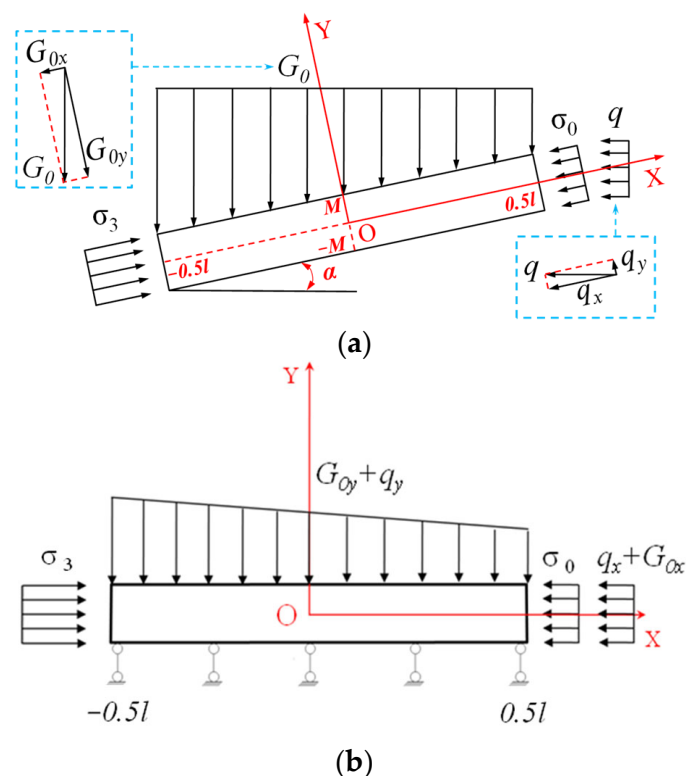


Figure 2. Mechanical model of elastic barrier zone of inclined waterproof coal pillar. (a) Mechanical simplified model and stress decomposition, (b) Stress characteristics of model after clockwise rotation α angle.

Through the above elaboration, we can analyze stress characteristics in the elastic barrier zone of the inclined waterproof coal pillar. As shown in Figure 2a, G_0 can be decomposed into G_{0x} and G_{0y} , and q can be decomposed into q_x and q_y . So the stress of G_{0x} and q_x is the horizon vector, and the stress of G_{0y} and q_y is the vertical vector. Thus,

$$G_0 = -K_1\gamma(H - x \sin \alpha), \tag{1}$$

$$G_{0y} = -K_1\gamma(H - x \sin \alpha)\cos\alpha, \tag{2}$$

$$G_{0x} = -K_1\gamma(H - x \sin \alpha)\sin\alpha, \tag{3}$$

$$q_x = -|q| \cos \alpha, \tag{4}$$

$$q_y = |q| \sin \alpha. \tag{5}$$

Because the vertical stress of EBZ does not change along with the change in Y-axis direction stress, G_0 is constant.

Thus, using the semi-inverse solution of elastic mechanics, this problem can be solved. In Figure 2a,

$$\sigma_y = G_{0y} + q_y = \frac{K_1\gamma \sin 2\alpha}{2}x + (|q|\sin\alpha - K_1\gamma H \cos \alpha). \tag{6}$$

To simplify the calculation, the following can be defined: $A = \frac{K_1\gamma \sin 2\alpha}{2}$, $B = |q| \sin \alpha - K_1\gamma H \cos \alpha$.

Therefore, according to the equilibrium differential equation, $\sigma_y = \frac{\partial^2 f(x,y)}{\partial x^2}$.

By integrating Equation (6), the stress function can be obtained:

$$f(x,y) = \int \sigma_y dy = \frac{A}{6}x^3 + \frac{B}{2}x^2 + f_1(y)x + f_2(y). \tag{7}$$

We can find that $f_1(y)$ and $f_2(y)$ are functions of the unknown parameter y . In order for the stress function $f(x, y)$ to hold, the compatibility equation should be satisfied:

$$\frac{\partial^4 f(x, y)}{\partial x^4} + 2 \frac{\partial^4 f(x, y)}{\partial x^2 \partial y^2} + \frac{\partial^4 f(x, y)}{\partial y^4} = 0. \tag{8}$$

Equation (7) is substituted into Equation (8) to obtain the following:

$$x \frac{\partial^4 f_1(y)}{\partial y^4} + \frac{\partial^4 f_2(y)}{\partial y^4} = 0. \tag{9}$$

Since $x \in [-0.5l, 0.5l]$, taking different values of x and substituting them into Equation (4) and simplifying it gives the following:

$$\frac{\partial^4 f_1(y)}{\partial y^4} = 0, \frac{\partial^4 f_2(y)}{\partial y^4} = 0.$$

Therefore, the expressions of $f_1(y)$ and $f_2(y)$ can be obtained:

$$f_1(y) = C_1 y^3 + C_2 y^2 + C_3 y + C_4, \tag{10}$$

$$f_2(y) = D_1 y^3 + D_2 y^2 + D_3 y + D_4. \tag{11}$$

By substituting Equations (10) and (11) into Equation (7), it is apparent that

$$f(x, y) = \frac{A}{6} x^3 + \frac{B}{2} x^2 + x(C_1 y^3 + C_2 y^2 + C_3 y + C_4) + (D_1 y^3 + D_2 y^2 + D_3 y + D_4). \tag{12}$$

This leads to

$$\sigma_x = \frac{\partial^2 f(x, y)}{\partial y^2} = 6C_1 xy + 2C_2 x + 6D_1 y + 2D_2, \tag{13}$$

$$\sigma_y = \frac{\partial^2 f(x, y)}{\partial x^2} = Ax + B, \tag{14}$$

$$\tau_{xy} = -\frac{\partial^2 f(x, y)}{\partial x \partial y} = -(3C_1 y^2 + 2C_2 y + C_3). \tag{15}$$

The elastic zone of the coal pillar is in critical equilibrium, and there is large interlayer friction between the coal and rock seams. Therefore,

$$\sigma_3 = -(\sigma_0 + q_x + G_{0x}). \tag{16}$$

Based on this simplified calculation, the symmetry of the mechanical model is therefore considered first. As shown in Figure 2b, since the bottom of the coal pillar can be regarded as a fixed-end constraint, the load on the elastic barrier zone of the waterproof coal pillar is symmetric along the XOZ side, so it should satisfy $\sigma_x(-y) = \sigma_x(y)$, $\sigma_y(-y) = \sigma_y(y)$, and $-\tau_{xy}(y) = \tau_{xy}(-y)$. Substituting this into Equations (13)–(15) yields $C_1 = D_1 = C_3 = 0$.

At this point, considering the boundary conditions, as shown in Figure 2b, at the boundary $x = -0.5l$, the following can be obtained:

$$\sigma_x(-0.5l) = -C_2 l + 2D_2 = -(\sigma_0 + q_x + G_{0x}). \tag{17}$$

At the boundary $x = 0.5l$, it follows that

$$\sigma_x(0.5l) = C_2 l + 2D_2 = \sigma_0 + q_x + G_{0x}. \tag{18}$$

The union of (17) and (18) is solved by $D_2 = 0$ and $C_2 = \frac{\sigma_0 + q_x + G_{0x}}{l}$, and combined with Equations (13)–(15), we can obtain the following:

$$\sigma_x = 2 \frac{\sigma_0 + q_x + G_{0x}}{l} x, \tag{19}$$

$$\sigma_y = G_{0y} + q_y, \tag{20}$$

$$\tau_{xy} = -2 \frac{\sigma_0 + q_x + G_{0x}}{l} y. \tag{21}$$

In the formula, $x \in [-0.5l, 0.5l]$ and $y \in [-0.5M, 0.5M]$.

Since the force in the horizontal direction of the coal pillar (with the coordinate axis as the reference system) is symmetrical along the Y -axis and the object has been assumed to be a uniform medium, the horizontal combined stress at the point O at its form center should be 0 and should only be subjected to pressure in the vertical direction. At this time, $x = 0$ and $y = 0$ are substituted into Equations (19)–(21), and σ_x and τ_{xy} are both 0, thus verifying the accuracy and reasonableness of the above equation.

The magnitude of the principal stress at any point within the elastic barrier of the coal pillar can be obtained by combining the elastodynamic principal stress relationship equations.

At this point, considering the underground engineering problem, the damage of the surrounding rock is suitable for analysis using the Mohr–Coulomb criterion, so the expression for the stress at its critical damage is introduced:

$$\sigma_1 = \frac{1 + \sin \varphi}{1 - \sin \varphi} \sigma_3 + \frac{2c \cos \varphi}{1 - \sin \varphi}. \tag{22}$$

By transforming the positions of σ_1 and σ_3 , the following can be obtained:

$$\sigma_3 = \frac{1 - \sin \varphi}{1 + \sin \varphi} \sigma_1 - \frac{2c \cos \varphi}{1 + \sin \varphi}. \tag{23}$$

According to the previous hypothesis, when the elastic barrier zone is critically damaged, the maximum principal stress σ_1 is $K_1 \gamma H$, which can be obtained as follows:

$$\sigma_3 = \frac{1 - \sin \varphi}{1 + \sin \varphi} K_1 \gamma H - \frac{2c \cos \varphi}{1 + \sin \varphi}, \tag{24}$$

where c is the cohesion of the coal body, and φ is the friction angle within the coal body.

Combined with the relationship between σ_1 and σ_3 and σ_x and σ_y in the Mohr–Coulomb criterion, the following can be obtained:

$$\sigma_1 = \frac{\sigma_x + \sigma_y}{2} + \sqrt{\left(\frac{\sigma_x - \sigma_y}{2}\right)^2 + \tau^2_{xy}}, \tag{25}$$

$$\sigma_3 = \frac{\sigma_x + \sigma_y}{2} - \sqrt{\left(\frac{\sigma_x - \sigma_y}{2}\right)^2 + \tau^2_{xy}}. \tag{26}$$

At this time, combined with Equations (19)–(21), the critical size of the elastic barrier zone can be obtained by substituting any point, σ_x , σ_y , or τ_{xy} , at the boundary of the waterproof coal pillar into Equations (22), (25) and (26). To simplify the calculation, the boundary point $(0, 0.5M)$ is substituted, as shown in Figure 2b, where $x = 0$ and $y = 0.5M$ (M is the thickness of the coal seam), which can be obtained as follows:

$$l = \frac{2M(K_1 \gamma H \sin \alpha + |q| \cos \alpha + |\sigma_0|)}{\sqrt{\left| [4c \cos \varphi + 2(|q| \sin \alpha - K_1 \gamma H \cos \alpha) \sin \varphi]^2 - (|q| \sin \alpha - K_1 \gamma H \cos \alpha)^2 \right|}}. \tag{27}$$

Equation (27) is the expression of the critical size of the elastic barrier zone of the inclined coal pillar (inclination angle α) under the influence of water pressure q and recovery disturbance (to reflect the directionality of the force more intuitively, the force in the negative direction with the coordinate axis is therefore added to the absolute value).

And when the coal seam dip angle is 0° , it is known that $\sin\alpha = 0$ and $\cos\alpha = 1$. The critical size l of the barrier zone in the middle of the waterproof coal pillar of the horizontal coal seam can be obtained by bringing in Equation (27):

$$l' = \frac{2M(|q| + |\sigma_0|)}{\sqrt{|(4c \cos \varphi - 2K_1\gamma H \sin \varphi)^2 - (K_1\gamma H)^2|}} \quad (28)$$

2.3. Calculation of the Critical Length of the Elastic Barrier

Based on the characteristics of the overburden load on the inclined waterproof coal pillar, combined with the functional relationships between various physical parameters and the above derivation process, the following is apparent:

- (1) The numerator of Equation (22), $K_1\gamma H \sin\alpha + |q| \cos\alpha + |\sigma_0|$, is exactly the main stress σ_x applied to both sides of the boundary of the elastic barrier zone of the coal pillar, and the denominator, $|q| \sin\alpha - K_1\gamma H \cos\alpha$, is the main stress σ_y applied to the upper boundary of the elastic zone of the coal pillar, while the rest are the mechanical parameters of the coal pillar and its dip angle. It can be seen that the critical length of the central barrier zone is closely related to the principal stress σ_x in the inclination of the elastic zone of the coal pillar, the principal stress σ_y in the vertical direction, and the inclination angle of the coal seam.
- (2) By analyzing Equations (19)–(21) and comparing them with Equation (27), we can see that when the dip angle of the seam is 0° , the forces at the bottom angle of the pillar are equal and maximum, and damage can occur at any position at the bottom of the pillar. When the inclination angle α is not 0° , the internal stresses in the pillar are greater at the corners, but the stresses at the lowest horizontal part of the pillar (e.g., the lower left corner of the pillar in Figure 2) are the greatest, and σ_x , σ_y , and τ_{xy} are the maximum values at this time. Therefore, when the load on the inclined coal pillar exceeds its limit, the lowest horizontal bottom angle of the pillar should be the most vulnerable to damage.
- (3) In the range of inclination angle $\alpha \in [0^\circ, 90^\circ]$, as the inclination angle increases, the load given to the coal pillar by the residual support pressure G_0 along the inclination of the seam gradually increases, while the load perpendicular to the coal pillar gradually decreases, i.e., σ_x is proportional to the inclination angle α , and σ_y is inversely proportional to the inclination angle α . Combined with Equation (27), we can deduce that the critical size of the elastic barrier zone of the waterproof coal pillar presents a characteristic proportional to the inclination angle of the coal seam.
- (4) The destructive effect of water on the coal pillar is mainly reflected in two aspects. On the one hand, there is the pressure effect on the coal pillar, as can be seen from Equations (27) and (28), with the increase in water pressure q , mainly reflected in the influence of the main stress σ_x on the tendency of the coal pillar, where the greater the water pressure is, the greater the critical length is. The other side is that the physical and mechanical properties of the coal rock body under water immersion will be significantly reduced, which will also affect the determination of the critical length of the elastic barrier zone of the waterproof coal pillar.

2.4. Determination of the Critical Size of MDZ and WAZ

The lengths of the mining disturbance zone (MDZ) and water pressure-affected zone (WAZ) are determined to be l_1 and l_0 . There are extremely well-established results to draw on for the study of the critical size of the coal pillars disturbed by mining at the working face. The literature [13,51] gives an expression for the critical size of the waterproof coal

pillar mining disturbance zone (MDZ) by applying the Mohr–Coulomb criterion, which has been tested in a wide range of applications:

$$l_1 = \frac{M}{2f\lambda} \ln \left| \frac{fK_1\gamma H + c}{(\lambda - 1)fc \cot \varphi + c} \right|, \tag{29}$$

where f is the friction factor between the top and bottom of the coal seam (generally, $f = \tan\varphi/4$), and λ is the lateral pressure coefficient, generally taking the value of 2.5.

As for the formula for calculating the length of the water pressure-affected zone in inclined coal seams, the literature [52] combined theoretical and empirical formulas and gave its ratio to the length of the recovery disturbance zone:

$$\frac{l_1}{l_0} = \frac{\cos(\delta + \alpha)}{\cos(\delta - \alpha)}, \tag{30}$$

where α is the coal pillar inclination angle, and δ is the rock seam movement angle.

Therefore, by combining Equations (27)–(30), a final equation for the critical length of the waterproof coal pillar in an inclined coal seam can be obtained:

$$L = l_1 + l + l_0 = \left[1 + \frac{\cos(\delta - \alpha)}{\cos(\delta + \alpha)} \right] \frac{M}{2f\lambda} \ln \left| \frac{fK_1\gamma H + c}{(\lambda - 1)fc \cot \varphi + c} \right| + \frac{2M(K_1\gamma H \sin \alpha + |q|\cos \alpha + |\sigma_0|)}{\sqrt{|4c \cos \varphi + 2(|q| \sin \alpha - K_1\gamma H \cos \alpha) \sin \varphi|^2 - (|q| \sin \alpha - K_1\gamma H \cos \alpha)^2}} \tag{31}$$

3. Application of Critical Size Calculation for the Waterproof Coal Pillar

3.1. Project Overview of the Study Area

This 18 m coal pillar has been left between the empty area of the 1301 working face and the auxiliary transport roadway of the current 1303 working face in Dananhu No. 1 Mine. As a result of the fissures generated by the mining disturbance during the mining process of the upper section (1301 working face), part of the coal pillar in the section (745–1114 m section from the return wind tunnel) is affected by water accumulation in the mining void area (Figure 3), where the accumulation elevation is +209 m, it is non-flow dynamic, and the maximum hydrostatic pressure is 0.26 MPa. Therefore, it is important to determine the limit of stability of the water-insulated coal pillar so as to predict whether the existing pillar can ensure the safe recovery of the working face under the influence of water.

Through multiple means, including field collection, coal rock sampling experiments, and physically similar simulations [51,53], the relevant parameters required for the waterproof coal pillar calculation were finally obtained (as shown in Table 1).

Table 1. Physical and mechanical parameters of coal pillar in Dananhu No. 1 Mine.

Elastic Zone Stress Concentration Factor K_1	Plastic Zone Stress Concentration Factor K	Dip Angle of Coal Seam α (°)	Coal Seam Thickness M (m)	Rock Volume Force γ (kN/m ³)	Buried Depth H (m)
2	4	12	6.5	24.5	255.5
Internal friction angle φ (°)	Cohesion c (MPa)	Poisson ratio ν_0	Maximum hydrostatic pressure q (MPa)	Strata movement angle δ (°)	Friction factor f
27.4	1.92	0.36	0.26	50	0.129

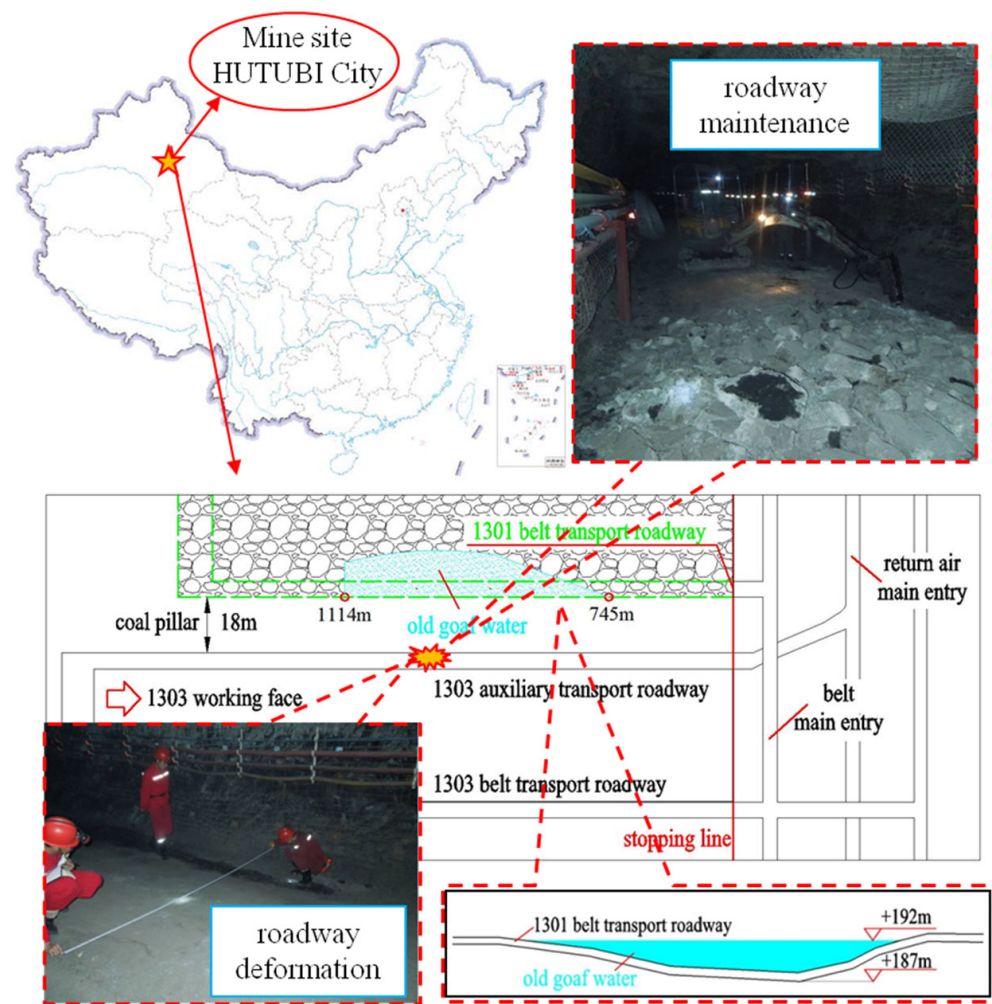


Figure 3. 1303 working face mining schematic diagram.

3.2. Calculation of the Critical Size of the Waterproof Coal Pillar in the Study Area

Substituting the above parameters into Equation (29), we can obtain the critical size l_1 of 2.95 m for the disturbance zone of the waterproof coal pillar. Then, from Equation (30), we can obtain the critical size l_0 of 4.95 m for the water pressure influence zone.

Substituting the above dimensional results and related parameters into Equation (24), the stress σ_0 at the junction of the plastic and elastic zones can be obtained as 6.921 MPa.

Finally, by substituting all the relevant parameters into Equation (27), the critical size l of the elastic barrier zone of the coal pillar in the limit state can be obtained as follows:

$$l = \frac{2M(K_1\gamma H \sin \alpha + |q|\cos \alpha + |\sigma_0|)}{\sqrt{[4c \cos \varphi + 2(|q| \sin \alpha - K_1\gamma H \cos \alpha) \sin \varphi]^2 - (|q| \sin \alpha - K_1\gamma H \cos \alpha)^2}} = 11.19 \text{ m}$$

$$= \frac{2 \times 6.5 \times (2 \times \frac{24.5 \times 255.5}{10^3} \times 0.208 + 0.26 \times 0.978 + 6.921)}{\sqrt{[4 \times 1.92 \times 0.8878 + 2 \times (0.26 \times 0.208 - 2 \times \frac{24.5 \times 255.5}{10^3} \times 0.978) \times 0.46]^2 - (0.26 \times 0.208 - 2 \times \frac{24.5 \times 255.5}{10^3} \times 0.978)^2}}$$

Therefore, in the limit state, the critical size of the inclined-state waterproof coal pillar is

$$L = l_1 + l + l_0 = 2.95 + 11.19 + 4.95 = 19.09 \text{ m.}$$

When the coal seam inclination angle α is assumed to be 0° , the critical dimensions of the elastic barrier zone l' and the water pressure influence zone l'_0 of the horizontal state coal pillar can be obtained by substituting Equations (28) and (30) as follows:

$$l' = \frac{2M(|q| + |\sigma_0|)}{\sqrt{|(4c \cos \varphi - 2K_1 \gamma H \sin \varphi)^2 - (K_1 \gamma H)^2|}} = \frac{2 \times 6.5 \times (0.26 + 6.921)}{\sqrt{|(4 \times 1.92 \times 0.8878 - 2 \times 2 \times \frac{24.5 \times 255.5}{10^3} \times 0.46)^2 - (2 \times \frac{24.5 \times 255.5}{10^3})^2|}} = 7.76 \text{ m},$$

$$l'_0 = \frac{\cos(\delta - 0^\circ)}{\cos(\delta + 0^\circ)} = l_1 = 2.95 \text{ m}.$$

At this time, the critical size of the horizontal state waterproof coal pillar is

$$L' = l'_1 + l + l'_0 = 2.95 + 7.76 + 2.95 = 13.66 \text{ m}.$$

Therefore, taking the geological conditions of Dananhu No. 1 Mine as the benchmark, the theoretical limit size is 13.66 m when the coal seam inclination angle α leaving the waterproof coal pillar is assumed to be 0° ; with the coal seam inclination angle α of 12° leaving the waterproof coal pillar, the width of the coal pillar is 19.09 m, an increase of 29%. The coal seam inclination angle has an extremely important influence on the retention of coal pillars. The width of the coal pillar left at the project site is 18 m, which is close to the limit size, so it is necessary to take corresponding measures to protect the coal pillar and the surrounding roadway.

4. Elastic–Plastic Evolution of the Waterproof Coal Pillar in the Study Area

4.1. Numerical Modeling of the Study Area

Flac3D 3.0, which was developed by the ITASCA company in Minneapolis, MN, USA, was used to study the elastic–plastic evolution process of the inclined coal pillar under the action of asymmetric load in this paper. Based on the geological conditions of the Dananhu No. 1 Mine, a numerical calculation model was established, as shown in Figure 4. Based on the field exploration and rock mechanics experiments, the relevant mechanical parameters were optimized and assigned, and the physical and mechanical parameters [53] of each rock seam are shown in Table 2.

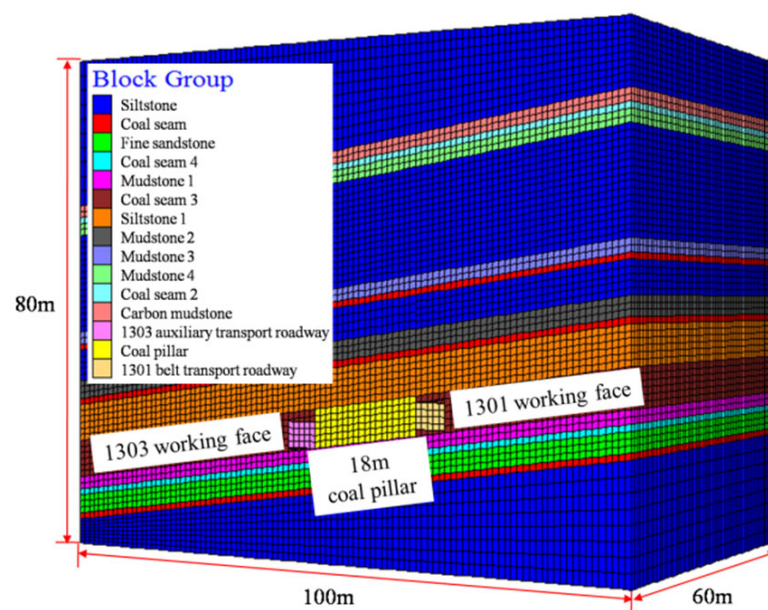


Figure 4. Numerical calculation model.

Table 2. Physical and mechanical parameters of the layers of Dananhu No. 1 Mine.

Layer	Compressive Strength (MPa)	Rock Density (kg/m ³)	Bulk Modulus (GPa)	Shear Modulus (GPa)	Internal Friction Angle φ (°)	Cohesion c (MPa)	Poisson Ratio ν_0
Siltstone	1.46	2360	7.8	2.8	29.9	5.35	0.29
Fine sandstone	1.33	2259	6.8	2.4	30	4.2	0.34
Siltstone	1.46	2360	7.8	2.8	29.9	5.35	0.29
Coal seam	0.48	1370	4.4	0.5	27.4	1.92	0.36
Mudstone	1.37	2397	6.07	1.37	29	3.07	0.28
Carbon mudstone	1.35	2400	6.8	1.9	28.6	4.07	0.28

4.2. Fracture Evolution and Plastic Zone Formation Process in the Coal Pillar

Under such conditions, internal fissures in the coal pillar will gradually develop and expand, resulting in a reduction in the overall strength of the pillar and local plastic deformation. In the case of the inclined waterproof coal pillar, due to the influence of its inclination angle, the force in the coal pillar will not be symmetrically distributed along its center line, which will lead to stress concentration in some areas of the coal pillar, and eventually, strength deterioration will occur, firstly in the stress concentration area.

Figure 5 reflects the evolution of the transformation of the elastic and plastic zones within the inclined waterproof coal pillar during the mining process, as can be seen from the figure.

- (1) From Figure 5a,b, it can be seen that with the retrieval of the upper section of the working face (1301 working face) and the excavation of the roadway in this section, the internal stress equilibrium of the coal pillar is broken. The roof plate of the 01 working face mining goaf area is broken, forming residual supporting pressure along the coal seam tendency. Finally, a triangular plastic zone appears in the upper right corner of Figure 5b. At this time, the coal pillar was in a unilateral loaded state, and the fissures in the surrounding rock of the roadway on the loaded side extended and expanded, so the loose range of the surrounding rock of the roadway on the side of the coal pillar in the mining void area was about 1m larger than that of the roadway on the other side of the coal pillar, but at this time, most areas of the coal pillar were still elastic zones, indicating that the internal fissures of the coal pillar were less developed and had good stability under the unilateral loaded state.
- (2) The change process from Figure 5c,d shows that when the working face of this section (03 working face) is retrieved, the coal pillar is in the loaded state on both sides. At this time, the coal pillar experiences change from unilateral pressure to pressure on both sides, and the range of its plastic zone on both sides is further increased. However, due to the influence of the coal seam inclination angle, the loading on both sides of the coal pillar is not symmetrical, which leads to the lower left corner of the coal pillar becoming the residual support pressure concentration area; at this time, the residual support pressure not only affects the stability of the coal pillar but also the transfer along the coal seam floor. This, combined with the fact that the coal seam floor is mudstone with low strength, leads to the apparent development of fissures in the lower left corner of the coal pillar and the formation of a large plastic zone. This is also consistent with the theoretical calculation of the location of the first damage to the coal pillar. During the whole process of fracture evolution and plastic zone formation, the fractures in the surrounding rock of the roadway on both sides of the coal pillar also expanded to a certain extent, which led to a significant increase in the loosening of the roadway, indicating that the stability of the roadway was also significantly reduced under the influence of mining disturbance.
- (3) In the numerical simulation, the plastic zone of the coal pillar base plate is penetrated, so the plastic penetration zone will easily become the old goaf water seepage channel and eventually induce water damage. Therefore, it is necessary to carry out

corresponding old goaf water prevention and coal pillar reinforcement measures in advance to ensure the safe recovery of the working face.

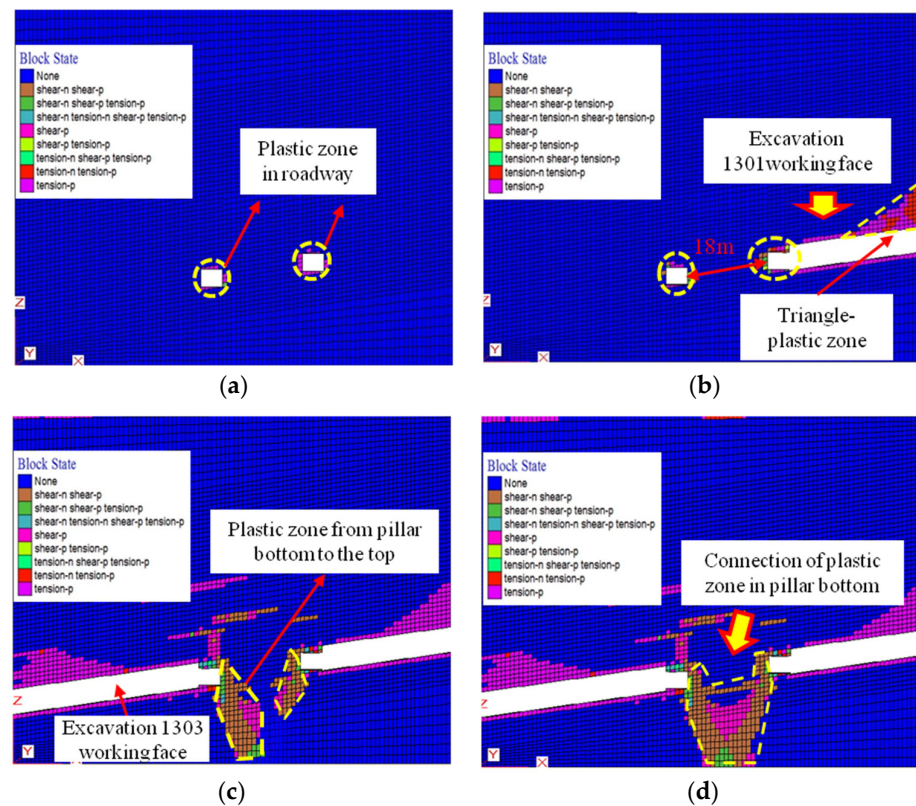


Figure 5. Evolution process of elastic–plastic zone in waterproof coal pillar after mining influence. (a) Excavation roadway, (b) excavation of 1301 working face, (c) model operation midway through excavation of 1303 working face and (d) model operation completed.

5. Engineering Practice

In view of the weakening of the coal pillar by the old goaf water and the characteristic that the bottom angle of the coal pillar is most easily damaged due to the inclination angle, secondary reinforcement of the waterproof coal pillar was carried out using pumping and pressure relief and grouting reinforcement in the area of serious deformation of the coal pillar.

5.1. Pumping and Pressure Relief

In order to achieve the pumping and pressure relief, four pumping holes were constructed from 11 September in the water pressure-affected area between 745 m and 1114 m in the 1303 auxiliary transport roadway (the horizontal elevation of the roadway in this area is between 183 and 202 m) in the mining area. The locations of the four pumping holes are shown in Table 3.

Table 3. Layout position of pumping hole and drilling parameters in goaf water-affected area.

Pumping Holes	Horizontal Elevation	Hole Position near Return Air Roadway	Drilling Parameters
ZK-321	201 m	818 m	Drilling depth is 19 m, drilling diameter is 52 mm
ZK-322	192 m	891 m	
ZK-323	187 m	964 m	
ZK-324	199 m	1037 m	

The water pressure of the old goaf water measured by the borehole during the pumping process is shown in Figure 6. As can be seen from the graph, the rate of decrease in water pressure shows a gradual decrease in the process of decreasing the volume of old goaf water. This is due to the fact that as the pumping works progress, the water pressure measured in each borehole also approaches 0 in turn, and, therefore, when a borehole has finished pumping and is sealed (1 m concrete seal), the total daily volume of water pumped out will decrease. Ultimately, as of October 2016, a total of 12,222 m³ of water had been pumped from the Dananhu No. 1 Mine, and the water pressure measured at the completion of the works was 0.028 MPa, indicating that this area contains only a very small amount of old goaf water.

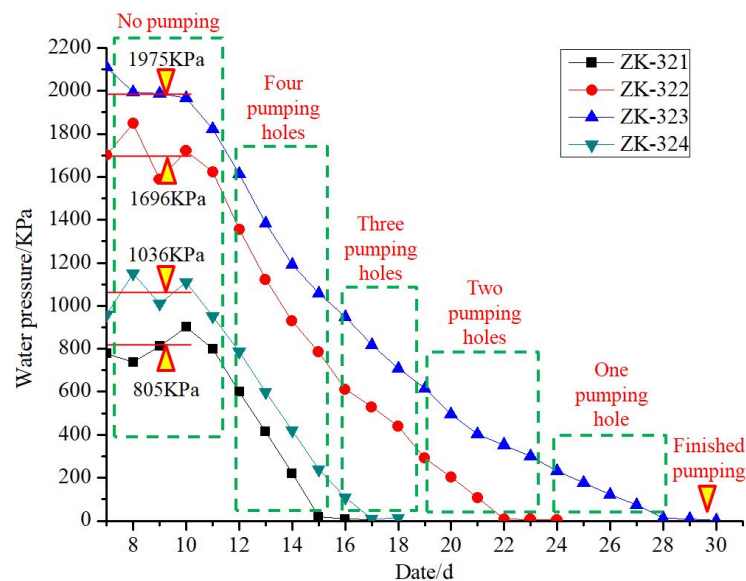


Figure 6. Water pressure measurement curve after pumping.

5.2. Grouting Reinforcement

Due to the obvious bottom drum and flaky gang phenomenon in the 1303 auxiliary transport roadway in the old goaf water-affected area during the working face mining period, the bottom plate drums out obviously near the coal pillar side, as shown in Figure 7a. Therefore, in order to reduce the further expansion of the plastic deformation area of the waterproof coal pillar, polyamine gum grease was injected into the serious plastic deformation area on the coal pillar side of the tunnel for the purpose of closing the fissures in the surrounding rock and ensuring the structural stability of the coal pillar, as shown in Figure 7b.

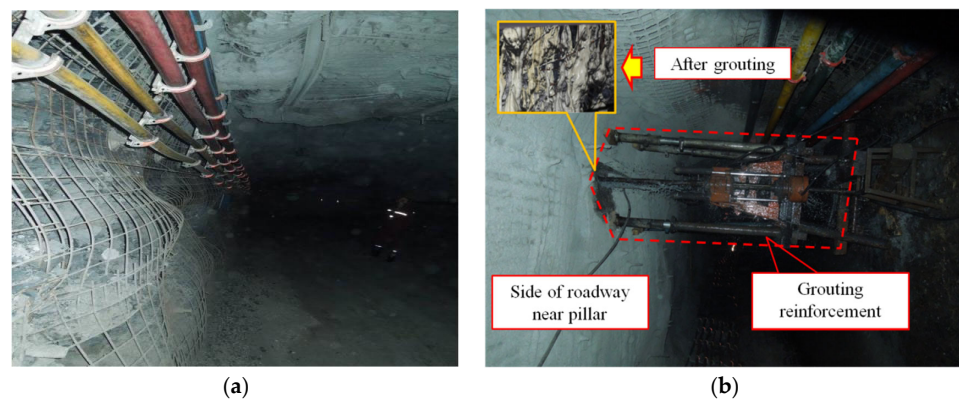


Figure 7. Grouting reinforcement by polyamine gum grease. (a) Tunnel bottom drum, (b) grouting reinforcement by polyamine gum grease.

As the bottom corner of the coal pillar is the starting point of plastic deformation expansion, a 42 mm diameter borehole with a depth of 5 m was constructed along a 45° downward direction from the coal pillar gang to inject Malisan (a mixture of polyamine grease and catalyst). The polyamine gum grease resin was mixed with the catalyst at a ratio of 1:1 and then injected into the coal pillar using a special polyamine gum grease grouting pump at a pressure of 8.0–18.0 MPa.

5.3. Effectiveness Test

Figure 8 reveals the deformation pattern of the surrounding rock of the coal pillar in the affected area of the old goaf water after taking corresponding measures. The deformation of the top and bottom plates of the roadway near the coal pillar and the two sides of the roadway were analyzed in chronological order, and the overall deformation rate of the coal pillar side of the roadway showed a decreasing trend. The second stage was the period of pumping and pressure relief and polyamine gum grease injection (8 September–28 September), when the three deformation rates of the roadway were significantly reduced by 5.6 mm/d for the top and bottom plates, 3.5 mm/d for the central two sides, and 2.5 mm/d for the lower two sides. The last stage was the post-reinforcement monitoring period (29 September–9 November), when the three deformation rates of the roadway were significantly reduced, with an average of 0.84 mm/d.

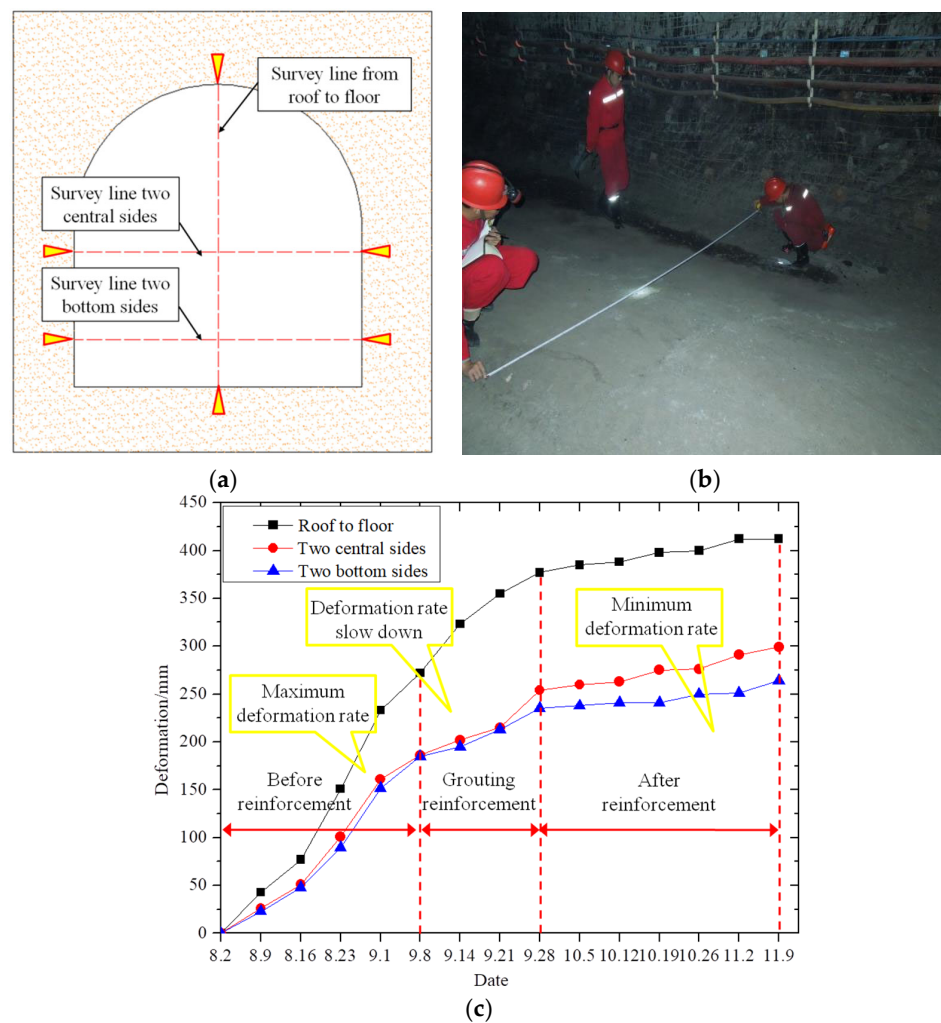


Figure 8. Effectiveness test of roadway near the coal pillar. (a) Survey line, (b) field monitoring, (c) deformation analysis of the roadway near the coal pillar.

Through the above analysis, it can be concluded that the old void water control and coal pillar reinforcement measures have effectively curbed the expansion of rock deformation surrounding the coal pillar and roadway, thus ensuring the safe recovery of the working face.

6. Conclusions

The paper conducts a mechanical analysis and numerical simulation study on the stability characteristics of the inclined waterproof coal pillar in Xinjiang mining areas under the influence of old goaf water. The findings are crucial for the safe extraction of coal resources and the promotion of a stable energy supply in China. The specific research outcomes include the following:

- (1) A mechanical model for the elastic barrier zone of the inclined waterproof coal pillar was established, and expressions for the critical dimension under asymmetric loading were derived. The study indicates that the limit dimension of the inclined waterproof coal pillar is significantly influenced by the angle of inclination. In scenarios where other geological factors remain constant, the critical dimensions of the elastic barrier zone in the inclined waterproof coal pillar show a direct proportional relationship with the coal seam inclination. Taking the geological conditions of Dananhu No. 1 Mine as an example, the critical width of the waterproof coal pillar at a 12° inclination increased by 30% compared to when the inclination was 0° .
- (2) Through numerical simulations, the evolution of the elastic–plastic zones in the inclined waterproof coal pillar under multiple mining disturbances was analyzed. Through combination with the mechanical analysis, it was found that the lowest bottom angle of the coal pillar was the first to experience failure. Numerical simulation experiments showed that fractures first developed and expanded at the lowest point of the coal pillar, leading to widespread plastic yielding, after which the plastic zone at the bottom corner extended along the floor of the coal seam towards the other bottom corner, eventually creating a channel for old goaf water seepage through the interconnected plastic zone at both bottom corners of the coal pillar.
- (3) The study analyzed how stress concentration in the bottom corner regions of the coal pillar, caused by overburden, is key to triggering the deterioration of pillar structural stability. Based on this, methods such as pumping water to relieve pressure and grouting reinforcement were used to enhance the stability of the inclined waterproof coal pillar. Field practice has shown that these measures significantly reduce the deformation rate of the roadway near the coal pillar, indicating that when the coal pillar is at its critical dimensions, appropriate old goaf water prevention and stability reinforcement measures can effectively restrain the deformation of the coal pillar and surrounding rock, thus ensuring safe mining of the working face.

Author Contributions: Data curation, P.S.; formal analysis, H.G.; funding acquisition, X.L.; project administration, W.Y.; software, X.Y. and H.G.; validation, P.S.; writing—original draft, X.Y.; writing—review and editing, X.L. and X.Y. All authors have read and agreed to the published version of the manuscript.

Funding: This work was supported by the Major Program of the National Natural Science Foundation of China, grant number 52394191.

Data Availability Statement: The original contributions presented in the study are included in the article, and further inquiries can be directed to the corresponding author.

Acknowledgments: A special acknowledgement should be shown to the anonymous reviewers for their constructive and valuable comments. We thank them for taking time from their busy schedule to provide guidance.

Conflicts of Interest: The authors declare no conflicts of interest.

References

1. Dong, S.N. Some key scientific problems on water hazards frequently happened in China's coal mines. *J. China Coal Soc.* **2010**, *35*, 66–71.
2. Xie, H.P. Research review of the state key research development program of China: Deep rock mechanics and mining theory. *J. China Coal Soc.* **2019**, *44*, 1283–1305.
3. Li, A.; Ma, Q.; Lian, Y.; Ma, L.; Mu, Q.; Chen, J. Numerical simulation and experimental study on floor failure mechanism of typical working face in thick coal seam in Chenghe mining area of Weibei. *Environ. Earth Sci.* **2020**, *79*, 8839. [[CrossRef](#)]
4. Dong, L.; Tong, X.; Ma, J. Quantitative Investigation of Tomographic Effects in Abnormal Regions of Complex Structures. *Engineering* **2021**, *7*, 1011–1022. [[CrossRef](#)]
5. Gu, H.L.; Lai, X.P.; Tao, M.; Cao, W.Z.; Yang, Z.K. The role of porosity in the dynamic disturbance resistance of water-saturated coal. *Int. J. Rock Mech. Min. Sci.* **2023**, *166*, 105388. [[CrossRef](#)]
6. Michieka, N.M. Energy and the environment: The relationship between coal production and the environment in China. *Nat. Resour. Res.* **2014**, *23*, 85–98. [[CrossRef](#)]
7. Sun, J.P.; Qian, X.H. Analysis of coal mine accidents in China during 2004–2015. *Ind. Mine Autom.* **2016**, *42*, 1–5.
8. Xue, Y.; Ranjith, P.G.; Dang, F.; Liu, J.; Wang, S.; Xia, T.; Gao, Y. Analysis of deformation, permeability and energy evolution characteristics of coal mass around borehole after excavation. *Nat. Resour. Res.* **2020**, *29*, 3159–3177. [[CrossRef](#)]
9. Gu, H.L.; Lai, X.P.; Tao, M.; Momeni, A.; Zhang, Q.L. Dynamic mechanical mechanism and optimization approach of roadway surrounding coal water infusion for dynamic disaster prevention. *Measurement* **2023**, *223*, 113639. [[CrossRef](#)]
10. Gu, W.; Xu, D.; Wang, Y.; Miao, K.; Yao, S.; Zhang, H.; Han, Z. Research on the stability and water Isolation of waterproof coal pillars between adjacent working faces under the Influence of water ponding goaf-A case study. *Appl. Sci.* **2024**, *14*, 884. [[CrossRef](#)]
11. Wang, T.; Wei, Y. Influence of stress evolution of coal pillar under unilateral water pressure. In *Advances in Mineral Resources, Geotechnology and Geological Exploration*; CRC Press: Boca Raton, FL, USA, 2022; pp. 290–294.
12. Shang, H.F.; Ning, J.G.; Hu, S.C. Field and numerical investigations of gate road system failure under an irregular residual coal pillar in close-distance coal seams. *Energy Sci. Eng.* **2019**, *7*, 2720–2740. [[CrossRef](#)]
13. Shi, W.; Zhang, J.; Zhang, H.; Liu, Y. Structural division and determination of rational width for waterproof partition coal pillar. *Chin. J. Rock Mech. Eng.* **2017**, *36*, 1227–1237.
14. Cai, M.F. Key theories and technologies for surrounding rock stability and ground control in deep mining. *J. Min. Strat. Control Eng.* **2020**, *2*, 5–13.
15. Rezaei, M.; Hossaini, M.F.; Majdi, A. A time-independent energy model to determine the height of distressed zone above the mined panel in longwall coal mining. *Tunn. Undergr. Space Technol.* **2015**, *47*, 81–92. [[CrossRef](#)]
16. Shi, L.; Wang, Y.; Qiu, M.; Han, L.; Zhao, Y. Research on the required width of a fault waterproof coal pillar based on underground pressure control theory. *Arab. J. Geosci.* **2019**, *12*, 480. [[CrossRef](#)]
17. Mu, H.; Bao, Y.; Song, D.; Su, D. Investigation of strong strata behaviors in the close-distance multi-seam coal pillar mining. *Shock Vib.* **2021**, *42*, 1263275.
18. Xia, B.; Jia, J.; Yu, B.; Zhang, X.; Li, X. Coupling effects of coal pillars of thick coal seams in large-space stopes and hard stratum on mine pressure. *Int. J. Min. Sci. Technol.* **2017**, *27*, 965–972. [[CrossRef](#)]
19. Bukowski, P. Water hazard assessment in active shafts in upper Silesian coal basin mines. *Mine Water Environ.* **2011**, *30*, 302–311. [[CrossRef](#)]
20. Wang, R.; Bai, J.-B.; Yan, S.; Chang, Z.-G.; Wang, X.-Y. An innovative approach to theoretical analysis of partitioned width & stability of strip pillar in strip mining. *Int. J. Rock Mech. Min. Sci.* **2020**, *129*, 104301.
21. Liang, W.; Zhao, G.; Wang, X.; Zhao, J.; Ma, C. Assessing the rock burst risk for deep shafts via distance-based multi-criteria decision making approaches with hesitant fuzzy information. *Eng. Geol.* **2019**, *260*, 105211. [[CrossRef](#)]
22. Wang, S.; Li, X.; Wang, D. Mining-induced void distribution and application in the hydro-thermal investigation and control of an underground coal fire: A case study. *Process Saf. Environ. Prot.* **2016**, *102*, 734–756. [[CrossRef](#)]
23. Yang, H.; Guo, Z.; Chen, D.; Wang, C.; Zhang, F.; Du, Z. Study on reasonable roadway position of working face under strip coal pillar in rock burst mine. *Shock Vib.* **2020**, *2020*, 8832791. [[CrossRef](#)]
24. Chen, Y.; Zhao, G.; Wang, S.; Wu, H.; Wang, S. AA case study on the height of a water-flow fracture zone above undersea mining: Sanshandao Gold Mine, China. *Environ. Earth Sci.* **2019**, *78*, 122. [[CrossRef](#)]
25. Frith, R.; Reed, G. Limitations and potential design risks when applying empirically derived coal pillar strength equations to real-life mine stability problems. *Int. J. Min. Sci. Technol.* **2019**, *29*, 17–25. [[CrossRef](#)]
26. Bo, L.; Chen, Y.L. Risk assessment of coal floor water inrush from underlying aquifers based on GRA-AHP and its application. *Eng. Geol.* **2016**, *34*, 143–154.
27. Tan, Y.L.; Yu, F.H.; Chen, L. A new approach for predicting bedding separation of roof strata in underground coal mines. *Int. J. Rock Mech. Min. Sci.* **2013**, *61*, 183–188. [[CrossRef](#)]
28. Wang, R.; Yan, S.; Bai, J.; Chang, Z.; Zhao, T. Theoretical analysis of damaged width & instability mechanism of rib pillar in open-pit high wall mining. *Adv. Civ. Eng.* **2019**, *2019*, 6328702.
29. Liu, Q.; Xue, Y.; Ma, D.; Li, Q. Failure characteristics of the water-resisting coal pillar under stress-seepage coupling and determination of reasonable coal pillar width. *Water* **2023**, *15*, 1002. [[CrossRef](#)]

30. Yu, W.; Wang, W.; Wu, G.; Yu, X.; Peng, W. Three zones and support technique for large section incline shaft crossing goaf. *Geotech. Geol. Eng.* **2017**, *35*, 1921–1931. [[CrossRef](#)]
31. Zhang, L.; Lai, X.; Pan, J.; Shan, P.; Zhang, Y.; Zhang, Y.; Xu, H.; Cai, M.; Xi, X. Experimental investigation on the mixture optimization and failure mechanism of cemented backfill with coal gangue and fly ash. *Powder Technol.* **2024**, *440*, 119751. [[CrossRef](#)]
32. Wang, G.; Wu, M.; Wang, R.; Xu, H.; Song, X. Height of the mining-induced fractured zone above a coal face. *Eng. Geol.* **2017**, *216*, 140–152. [[CrossRef](#)]
33. Sun, W.; Zhang, S.; Guo, W.; Liu, W. Physical simulation of high-pressure water inrush through the floor of a deep mine. *Mine Water Environ.* **2017**, *36*, 542–549. [[CrossRef](#)]
34. Wang, S.; Huang, L.; Li, X. Analysis of rock burst triggered by hard rock fragmentation using a conical pick under high uniaxial stress. *Tunn. Undergr. Space Technol.* **2020**, *96*, 103195. [[CrossRef](#)]
35. Zhang, S.; Guo, W.; Li, Y.; Sun, W.; Yin, D. Experimental simulation of fault water inrush channel evolution in a coal mine floor. *Mine Water Environ.* **2017**, *36*, 443–451. [[CrossRef](#)]
36. Yu, Y.; Deng, K.-Z.; Luo, Y.; Chen, S.-E.; Zhuang, H.-F. An improved method for long-term stability evaluation of strip mining and pillar design. *Int. J. Rock Mech. Min. Sci.* **2018**, *107*, 25–30. [[CrossRef](#)]
37. Zhao, Y.; Peng, Q.; Wan, W.; Wang, W.; Chen, B. Fluid–solid coupling analysis of rock pillar stability for concealed karst cave ahead of a roadway based on catastrophic theory. *Int. J. Min. Sci. Technol.* **2014**, *24*, 737–745. [[CrossRef](#)]
38. Xie, X.F.; Li, X.B.; Shang, X.Y.; Weng, L.; Deng, Q. Prediction of height of water flowing fractured zone based on PCA-BP neural networks model. *China Saf. Sci. J.* **2017**, *27*, 100–105.
39. Yin, H.; Tang, R.; Xie, D.; Lang, N.; Li, S.; Zhang, X.; Cheng, Y.; Wang, S.; Li, A. Study on the evolution of fault permeability and the retention of coal(rock) pillar under the mining conditions of thick coal seam in the footwall of large normal fault. *ACS Omega* **2023**, *8*, 4187–4195. [[CrossRef](#)] [[PubMed](#)]
40. Russell, F.; Guy, R. Coal pillar design when considered a reinforcement problem rather than a suspension problem. *Int. J. Min. Sci. Technol.* **2018**, *28*, 11–19.
41. Liang, W.; Zhao, G.; Wu, H.; Chen, Y. Assessing the risk degree of goafs by employing hybrid TODIM method under uncertainty. *Bull. Eng. Geol. Environ.* **2019**, *78*, 3767–3782. [[CrossRef](#)]
42. Meng, X.G.; Liu, W.T.; Mu, D.R. Influence analysis of mining’s effect on failure characteristics of a coal seam floor with faults: A numerical simulation case study in the Zhaolou coal mine. *Mine Water Environ.* **2018**, *37*, 754–762. [[CrossRef](#)]
43. Liu, X.S.; Song, S.L.; Wu, B.Y.; Li, X.; Yang, K. Study on deformation and fracture evolution of underground reservoir coal pillar dam under different mining conditions. *Geofluids* **2022**, *2022*, 2186698.
44. Kumar, R.; Das, A.J.; Mandal, P.K.; Bhattacharjee, R.; Tewari, S. Probabilistic stability analysis of failed and stable cases of coal pillars. *Int. J. Rock Mech. Min. Sci.* **2021**, *144*, 104810. [[CrossRef](#)]
45. Fu, Q.; Yang, K.; Wei, Z.; He, X. Study on ultimate strength and dip effect of coal pillar in steeply dipping coal seam. *Geotech. Geol. Eng.* **2023**, *41*, 3447–3457. [[CrossRef](#)]
46. Lai, X.; Xu, H.; Shan, P.; Hu, Q.; Ding, W.; Yang, S.; Yan, Z. Research on mechanism of rockburst induced by mined coal-rock linkage of sharply inclined coal seams. *Int. J. Miner. Metall. Mater.* **2024**, *31*, 1–14.
47. Xu, H.; Lai, X.; Shan, P.; Yang, Y.; Zhang, S.; Yan, B.; Zhang, Y.; Zhang, N. Energy dissipation characteristics and shock mechanism of coal-rock mass induced in steeply-inclined mining: Comparison based on physical simulation and numerical calculation. *Acta Geotech.* **2023**, *18*, 843–864. [[CrossRef](#)]
48. Das, A.J.; Paul, P.S.; Mandal, P.K.; Kumar, R.; Tewari, S. Investigation of failure mechanism of inclined coal pillars: Numerical modelling and tensorial statistical analysis with field validations. *Rock Mech. Rock Eng.* **2021**, *54*, 3263–3289. [[CrossRef](#)]
49. Wang, Y.; Yao, D.X.; Lu, H.F. Elastic mechanics solution of water proof key layer in coal seam floor under high water pressure. *Coal Geol. Explor.* **2019**, *47*, 127–137.
50. Cai, M.F.; He, M.C.; Liu, D.Y. *Rock Mechanics and Engineering*; Science Press: Beijing, China, 2002.
51. Liu, C.W.; Ding, K.X. Research on critical size of water barrier in underground coal mine. *J. China Coal Soc.* **2001**, *26*, 632–636.
52. Wang, Z.Q.; Chen, C.F.; Wang, L.; Li, P.; Guo, X.; Gao, Y. Research on reasonable size of waterproof pillar in mining inclined coal seam. *J. Min. Saf. Eng.* **2013**, *30*, 735–738.
53. Lai, X.P.; Xu, H.C.; Kang, Y.L. Analysis on “spatio-tempo-intension” evolution rules of overburden strata movement in fully mechanized top-coal caving face. *J. Xi’an Univ. Sci. Technol.* **2018**, *38*, 871–877.

Disclaimer/Publisher’s Note: The statements, opinions and data contained in all publications are solely those of the individual author(s) and contributor(s) and not of MDPI and/or the editor(s). MDPI and/or the editor(s) disclaim responsibility for any injury to people or property resulting from any ideas, methods, instructions or products referred to in the content.